

Paper ID ICLASS06-107

INFLUENCE OF INJECTION NOZZLE PARAMETERS ON THE SPRAY PROPAGATION AND COMBUSTION IN A DI-DIESEL-ENGINE

Koch ¹, Schmid ² and Leipertz ³

¹ Ph.D. student, Dept. of Technical Thermodynamics (LTT), University of Erlangen-Nuremberg, pk@litt.uni-erlangen.de

² Ph.D. student, Dept. of Technical Thermodynamics (LTT), University of Erlangen-Nuremberg, ms@litt.uni-erlangen.de

³ Professor, Dept. of Technical Thermodynamics (LTT), University of Erlangen-Nuremberg, sek@litt.uni-erlangen.de

ABSTRACT In order to achieve a fast and comprehensive analysis of the influences of different engine parameters on the combustion process, a combination of five non-intrusive temporally and spatially highly resolving optical measurement techniques were applied simultaneously to a passenger car DI Diesel transparent engine. These measurement techniques include Mie scattering, laser-induced fluorescence, laser-induced incandescence and spectrally resolved flame luminosity. With these measurement techniques the influence of the nozzle geometry on spray formation, mixing, ignition, combustion and soot formation was examined. Besides significant influence on the spray break-up, the investigation also revealed the relevance of the combustion bowl wall on mixture formation and combustion.

Keywords: Optical Diagnostic, Simultaneous Measurements, Diesel Engine

1. INTRODUCTION

In times of decreasing oil resources and strongly increasing fuel costs economical engine concepts show great acceptance, especially if no losses concerning performance and driving comfort need to be accepted. This requirement profile corresponds exactly to the one of modern DI Diesel engines. This is the main reason for the ongoing increase of diesel driven cars in new vehicle registrations across Europe. Last official information from the Federal Bureau of Motor Vehicles and Drivers confirms that nearly 50 % of all new registered cars in Germany are powered by a diesel engine. With this increase the interest in the produced exhaust emission, especially soot and PM, awakes more public opinion and legislative restriction. At the moment this rising pressure results in the application of particulate filters as the favourite solution to reach new and stricter emission regulations. Whether the new limits will be reached with a filter system or not, it is obvious that further improvements of current engines concerning combustion and with it fuel consumption and pollutant emissions are necessary. In order to reach this target a deepened knowledge on the engine processes and their interaction is needed. By means of modern optical diagnostics it is possible to investigate these phenomena without influencing the complicated chemical reactions with high spatial and temporal resolution starting with the injection and ending with the soot oxidation process. Since these different processes influence each other significantly and relevant information may be lost if the single process steps are detected separately, in this investigation five optical measurement techniques were used simultaneously (four of them at the same time) in order to characterize the interacting chain of engine processes as comprehensive and detailed as possible. With this combination it is possible, to detect within one engine cycle the propagation of the liquid fuel phase by Mie scattering, the quality of mixture formation by laser-induced fluorescence (LIF), the ignition and lean combustion by detecting the flame luminosity in the UV

spectral range (FL_UV) and the rich sooting combustion by acquiring the signals of thermally excited soot in the visible spectral range (FL_VIS) as well as the characterization of the two-dimensional soot distribution inside the combustion chamber by laser-induced incandescence (LII). This combination of different measurement techniques allows a complete characterization of the influences of several engine and combustion relevant parameters on the processes inside the combustion chamber. In this paper especially the influence of different nozzle geometries on spray formation, mixing, ignition, combustion and soot formation was examined. Besides significant influence of the nozzle hole length, the investigation also revealed the relevance of the combustion bowl wall on mixture formation and combustion.

2. EQUIPMENT

2.1 Transparent Engine

The engine used in this study is a single-cylinder 4-Stroke transparent engine based on an AUDI V6 TDI series production engine. A short summary of important data is given in Table 1. For further information it will be referred to former publications. [1., 2.]

Table 1: Engine Data

Stroke / Bore	86.4 mm / 78.3 mm
Displacement	416 cm ³
Swirl (Tippelmann)	0,49
Connecting rod ratio	0,273
Compression	$\epsilon = 15.5$
Combustion chamber depth	10.55 mm
Combustion chamber diameter	48 mm

The transparent engine provides optical access to the combustion chamber from three sides. The cylinder head and the crank case are connected via an elongation device which carries side windows on the intake and outlet side of the engine. The piston crown has two windows which

permit the optical access into the combustion bowl. These windows are aligned in the direction of the side windows in the elongation element. The third access into the combustion chamber is through its bottom by means of a plane glass window. This plane window together with the straight walls of the combustion bowl forms a flat chamber with a bowl volume corresponding to the one of the series production engine. The piston is elongated and has a slot which allows the positioning of a detection mirror under the bottom window while the engine is operating. A depiction of the used transparent engine is shown in Figure 1

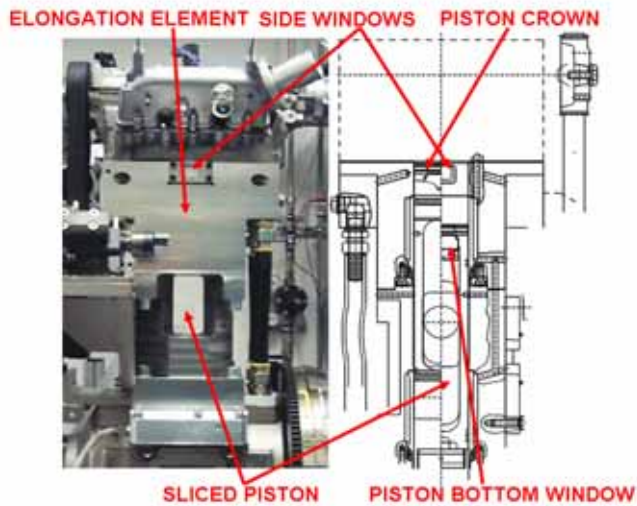


Figure 1: Transparent Engine

In comparison to the series production engine the piston rings were lowered to prevent their contact with the side windows of the elongation element. The resulting loss in the compression ratio is widely compensated by an external heatable boosting device. The heating of the engine oil and water permits investigations exceeding cold start conditions. In order to minimize soot fouling and mechanical stress of the optical accesses, the engine was operated in skip-fired mode. Only when the camera system is ready for recording, fuel was injected into the cylinder.

2.2 Injection System

For this investigation two multi-hole nozzles with different geometries were used. The used mini sac-hole-nozzles have 6 holes and double needle guide. Both nozzles have the same rated flow of $Q_{hyd} = 360\text{cm}^3/30\text{s}$ at 100 bar relative pressure and a spray angle of 160° without a slope angle. An overview over some important technical information is listed in Table 2.

Table 2: Nozzle data

Definition	Geometry of nozzle hole [°]	Nozzle hole length [mm]	Nominal hole diameter [mm]	Hydro-Grinding HG [%]
DLLA 906	k = 1,5	0,95	0,145	10,4
DLLA 727	k = 1,5	1,38	0,137	10,5

The engine is equipped with a passenger car common rail injection system which together with the nozzles and the injectors has been supplied by Robert Bosch GmbH.

3. MEASUREMENT TECHNIQUES

The combination of five different optical measurement techniques with two ICCD camera systems allowed the simultaneous measurements with maximum information at one crank angle within a single engine cycle. The experimental set-up for the used optical diagnostics and the transparent engine is sketched in Figure 2.

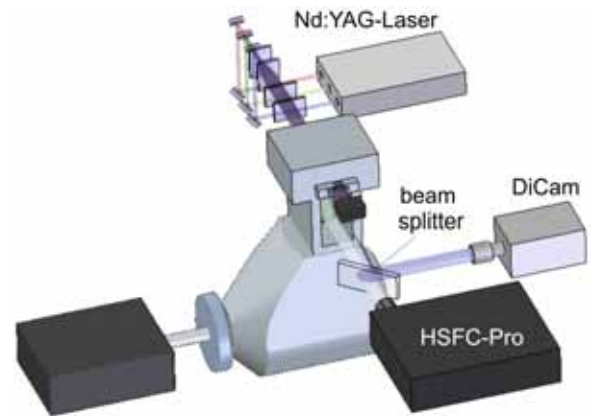


Figure 2: Schematic of the simultaneous optical diagnostics set-up

For the three laser-based measurement techniques (Mie scattering, LIF, LII) a Nd:YAG-Laser was used operating at three wavelengths simultaneously. The laser beams were guided into the combustion chamber by a light sheet optics which was optimized for LIF and LII and forms a light sheet of about 0.5 mm thickness. The light sheets could be adjusted in height according to the crank angle dependent piston position. The signals were detected over a decoupling mirror beyond the piston window by a combination of four independently gateable ICCD cameras of the same type. Three cameras are combined with a beam splitting optics within one housing (HSFC-Pro). The fourth camera (DiCam) for detecting the UV flame luminosity is optically separated from the other ones. Images were acquired in sets of 15 ones from 15 separate cycles. The images presented in the following have been averaged from these single image sets. In the following the use optical measuring techniques will be briefly presented, for further information it will be referred to the stated references.

3.1 Mie Scattering (Mie)

Mie scattering is based on the elastic scattering of light at phase interfaces and is used to detect the liquid fuel phase [3.]. For the signal excitation the frequency-doubled wavelength (532nm) of the Nd:YAG laser was used. The detection of the signals was conducted with one ICCD camera from the multiple camera system. The combination of these two components (Nd:YAG laser and ICCD camera) allows due to their specifications a high spatial and temporal resolution. Due to reflection and scattering of the laser light at the wall of the combustion bowl and in the dense fuel spray the liquid phase is integrally illuminated which permits the detection of the entire spray body for all

observation times.

3.2 Laser-induced Fluorescence (LIF)

LIF emits, after an absorption process to a higher electronic energy level of a molecule, fluorescence radiation at a wavelength which is equal or rather mostly larger than that one of the excitation light source. Due to this absorption process LIF is molecule specific [4.]. Thus detection of fuel, residual gas as well as smallest amounts (ppm) of combustion intermediates (OH) and pollutants (NO, CO, HC) is possible. For the present study the frequency-tripled wavelength (355nm) of a Nd:YAG-laser has been used to excite, e.g., polyaromatic hydrocarbons (PAH) of the fuel. The resulting fluorescence signal which is red-shifted occurs in a wavelength range between 380nm and 450nm and is also detected with an ICCD camera from the HSFC-Pro system. For this investigation LIF was used to visualize the successive propagation and distribution as well as the following burnout of the gaseous fuel. Since the resulting signals contain both liquid phase and vapour phase information, for the separation of both phases the liquid phase dependent Mie scattering signals have to be taken into consideration.

3.3 Spectrally resolved Flame Luminosity

The diesel combustion can be seen as a two stage process. At ignition a pre-mixed combustion process starts and after a short time period the process turns into a diffusive combustion. This very complex reaction mechanism has so far only been described numerically for n-heptan and isoctane. The simulation of the detailed reaction mechanism for the ignition of n-heptan in a homogeneous reactor revealed, that one of the first radicals appearing in significant concentration levels is the OH-radical. This theoretical work is supported by the works of Bertsch [5.] and Koyanagi [6.]. The highest OH-radical concentration can be found in areas where the fuel-air mixture is stoichiometric or slightly fuel lean. For a lean or stoichiometric premixed combustion the chemiluminescence of activated radicals (OH, CH, C₂) is the main source of luminosity [7.]. A fuel rich sooting combustion is also emitting light due to chemiluminescence but this emission is quite weak compared to the much more intense grey body radiation of the thermally excited soot especially in the visible range. Due to this situation, the detection of flame luminosity was split in two wavelength ranges, one in the visible range and one in the UV-range between 300 nm and 320 nm. At these wavelengths the most important emission source is the chemiluminescence of the OH-radical (308 nm) [7., 8.]. In this study the OH signal was detected with an UV-sensitive ICCD camera (DiCam) equipped with suitable filters. As described above, the OH-signal can be taken as marker for the ignition process. To use it also as identifier for lean or stoichiometric combustion one has to bear in mind that OH-radicals are also created in fuel rich combustion of hydrocarbons. Therefore, additional information on the flame is necessary. The necessary data can be derived from the detection of thermal soot radiation as soot is only formed during fuel rich combustion. For the detection of the thermally excited soot, the visible range is favourable. A comparison of the UV signals to those of the soot radiation permits the evaluation of the type of combustion. As the

chemiluminescence emissions in the visible range (chemiluminescence of CH; C₂; CN) of a lean premixed combustion are several orders of magnitude smaller than those of a rich sooting flame they can not be resolved if the camera sensitivity is set constant for all crank angles. Therefore, lean or stoichiometric combustion is only given for signals appearing only in the UV-range with no signals in the visible range. So, if signal at both cameras is detected fuel rich sooting combustion can be identified emitting over a wide spectral range. By evaluating the images of the spectrally resolved flame a statement on the quality of combustion [9.] is possible. Here in this investigation, the signals were detected in the wavelength range between 380 nm and 800 nm by another ICCD camera of the HSFC-Pro system. As the flame luminosity detection is a line of sight measurement the signals are integrated over the depth of the flame in detection direction.

3.4 Laser-induced Incandescence (LII)

The signal intensity of the thermally excited soot radiation in a flame depends on the temperature and the concentration of the soot particles. In contrast to this for LII the soot particles are heated up to their evaporation temperature (4000 to 4500 K) by a short high energetic laser pulse [10. - 12.]. Therefore, all soot particles in the measurement volume have about the same temperature and the strength of the emitted signal only depends on the soot volume concentration in the measurement volume [13.]. By using a laser light sheet the soot distribution can be resolved spatially as only the soot within the thin laser sheet is excited and the larger the acquired signal is the higher the soot concentration. The detection took place at a wavelength between 380 nm and 450 nm with a very short exposure time of 40 ns and was executed with the same ICCD camera of the HSFC-Pro system as was used for the LIF images. Dependent on the measurement technique optionally the 1064 nm (LII) or the 355 nm (LIF) beam was blocked by a shutter.

4. OPERATING POINTS

In this study the influence of a modification of the nozzle hole geometry on the spray propagation, evaporation, combustion and soot emission was investigated. For the researched points a reference diesel from Haltermann (RF-06-03) was used. The total amount of injected fuel for both operating points was 10 mg at a rail pressure of 800 bar. These adjusted conditions correspond to partial load operation of a real engine. The mean effective pressure for both investigated point is about 3.5 bar. The electrical start of the single main injection was set to 358 °CA. Both operating points were examined at an engine speed of 1500 rpm and a motored cylinder pressure of 55 bar. The temperature of the engine's oil and water circulation was kept constant at 85 °C. In the following the operating point 1 (OP1), nozzle 906, will be defined as reference and thus be used for comparison to operating point 2 (OP2) with nozzle 727.

5. RESULTS AND DISCUSSION

5.1 OP 1 (Nozzle 906)

For this operating point in Figure 3 the motored (green)

and fired cylinder pressures (blue) are displayed as well as the Rate of Heat Release (RoHR, red). Additionally also the course of the rail pressure (mint) and the injector current (marine), measured with a clamp-on ammeter, is shown. The Rate of Heat Release was calculated using simplified equations to have the possibility of comparing the operating points in advance. For this reason only the developing of the values is from importance and not their magnitudes.

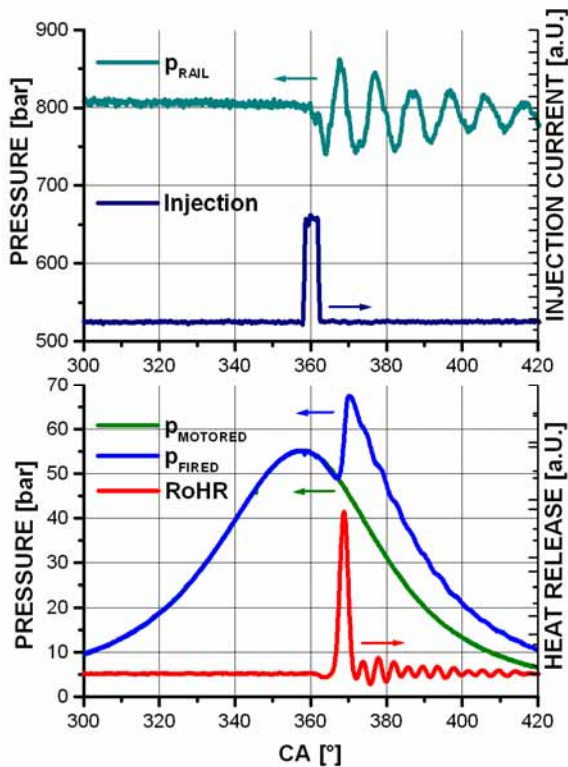


Figure 3: Indication data OP1

The presented curves, except the RoHR sequence, are taken from different working cycles within one observed crank angle and can be seen representative for all measurements for this operating point. One measured crank angle position consists of 80 working cycles, whereas only every sixth cycle fuel is injected and therefore “fired”. The temporal resolution of the engine indication is 0.1°CA which responds to approximately $11\ \mu\text{s}$ for a revolution speed of $1500\ \text{min}^{-1}$. The Rate of Heat Release was calculated from averaged and smoothed motored and fired pressure data from one working cycle. It can be used for an analysis of the combustion process and its quality in advance.

The decreasing part of the curve after 361°CA until 364°CA corresponds to the evaporation of the liquid fuel, as negative values represent the energy consumption necessary for the fuel evaporation. The ignition of the cylinder charge occurs at 365°CA up to 367°CA , derived from the first significant increase of the RoHR curve after the local minimum at 364°CA . The subsequent developing of the values (formation of a narrow peak) is characteristic for the behaviour of a pre-mixed burning reaction. Therefore the period where the predominant part of the combustion is lean extends in the region of 367°CA until 370°CA . The following periodical decay of the alternating curve progression marks the transition towards diffusive combustion and finally the burn-out of the cylinder charge.

Besides this exclusive conventional engine indication, the functioning chain of diesel combustion was also analysed by means of optical measuring techniques. Therefore the complete combustion process beginning with the visible start of injection until the burn-out of the cylinder charge was investigated with a resolution of 1°CA . This means that four, partly laser-based, optical measuring techniques were applied simultaneously to get the maximum amount of information at one crank angle position. Depending on actual state of combustion it was alternated between laser-induced fluorescence (spray propagation and mixture formation \rightarrow LIF) and incandescence (combustion and soot generation \rightarrow LII). Overlapping crank angles were measured for each method one after the other. In Figure 4 a composition of the results of the optical analysis in the form of a sequence of representative crank angle positions is shown. Beginning on the left side the average images of the Mie scattering, the flame luminosity in ultra-violet and visible spectral range as well as the ones of the laser-induced fluorescence in alteration with the laser-induced incandescence are shown.

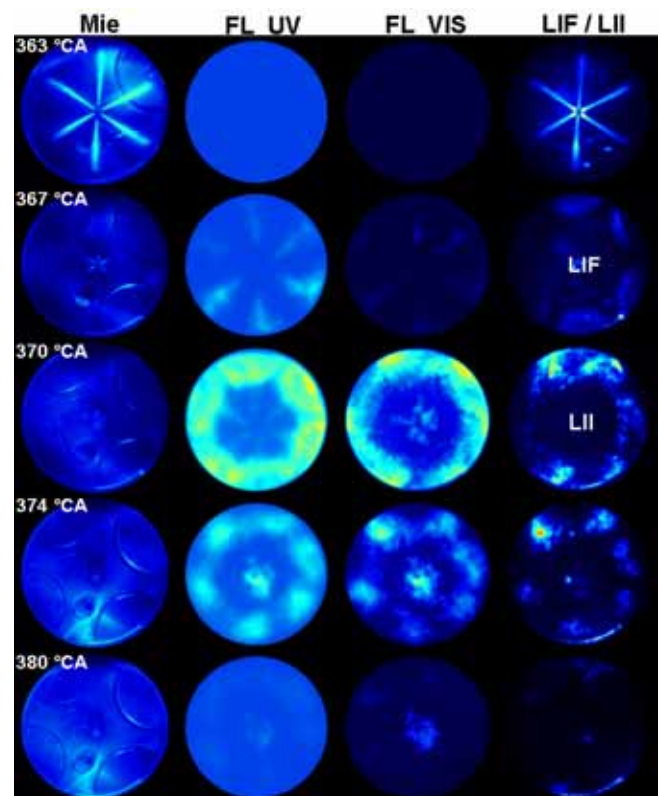


Figure 4: Sequence OP1

With a delay of 3°CA between electrical triggering and visible start of injection the first Mie signal appears at 361°CA for OP 1. At the same time the heat release curve shows a decrease and negative values as heat is needed for the evaporation of the injected liquid fuel. The Mie images show at 363°CA six spray cones of liquid fuel penetrating nearly symmetrically into the combustion chamber with a very small cone angle. Till the end of injection at 367°CA no significant wall contact of the liquid phase is visible. In contrast to that the LIF images show the formation of semicircular vapour propagation around the impingement points of the jets. Besides the fuel vapour spreading along

the wall (see LIF), there is due to the rebound from the wall also a movement back into the direction of the combustion bowl centre. The first visible signs for the ignition of the fuel-air-mixture can be seen at 366 °CA close to the combustion bowl wall in the middle of the vapour regions. At 367 °CA first signals of combustion, stronger in the ultra-violet and weaker in the visible spectral range, are observable along the axes of the injection jets. Until 370 °CA an increase in intensity of these signals, in both spectral ranges, and the formation of triangular regions in the outer area of the combustion bow can be observed. Due to the rising part of diffusive combustion and sooting spots a change towards laser-induced incandescence at the composition of the simultaneous measuring techniques was performed. Moreover a ring-shaped, lean combustion region in the outer area of the combustion bowl forms in which six diffusive combustion fragments are noticeable. The visible start of ignition correlates also very well with the heat release curve as can be seen in Figure 3. Starting at 370 °CA additional combustion signals of a diffusive flame can be observed close to the nozzle tip. A reason for that might be residual fuel from the nozzle sac hole, evaporating into the combustion chamber and causing this sooting combustion. With proceeding combustion an overlap of the spectrally resolved flame luminosity occurs and therefore a distinction into lean and rich combustion is with this technique no longer possible. Furthermore the spray impingement points at the combustion bowl wall are identified as the main sooting spots at 374 °CA via LII. After 380 °CA no combustion in the outer combustion bowl region can be detected, only the combustion signals close to the nozzle are still remaining.

5.2 OP 2 (Nozzle 727)

Figure 5 shows the indication data of this operating point gained via conventional measuring techniques.

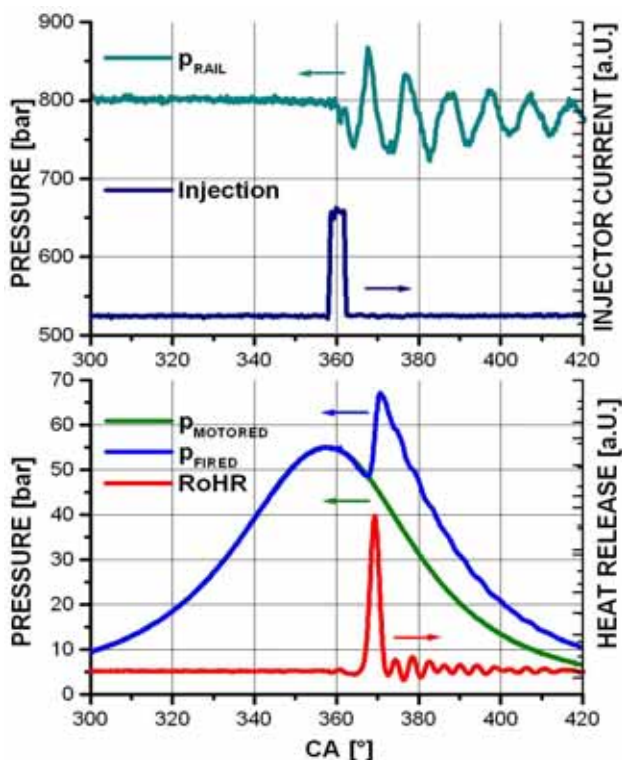


Figure 5: Indication data OP2

The developing of the rail and the motored pressure as well as the injection current values shows that the injection conditions for both operating points are practically identical. The evaporation decay of the RoHR course starts also at 361 °CA but extends compared to OP1 until 365 °CA and takes thus one crank angle more. Therefore there is an offset of 1 °CA for the subsequent developing of the heat release, whereas the graph itself is nearly identical to the one of OP1.

The results achieved with the simultaneous optical measuring technique for this operating point are presented in Figure 6. The structure of the sequence and the splitting of the images are abutted to the proceeding for OP1. At 363 °C the first significant difference in the spray propagation is observable. Due to the increase of the nozzle hole length the break-up of the spray cone shows a delay and hence an increase in penetration depth is achieved. However a definite impingement of liquid fuel on the combustion bowl wall can not be detected for this operating point. On the basis of the LIF signals a clearly more distinctive spreading of the fuel vapor phase along the combustion bowl wall becomes apparent.

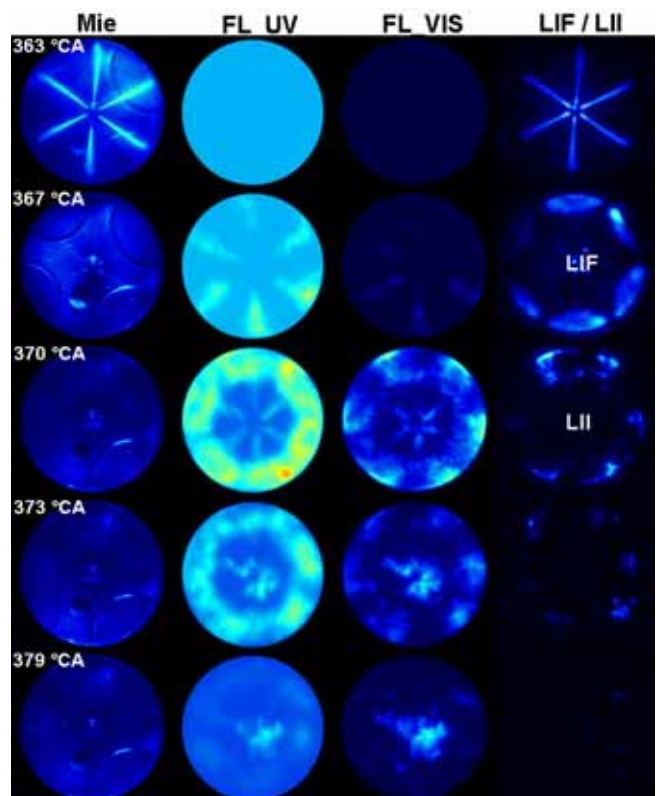


Figure 6: Sequence OP2

The first visible ignition reactions occurring at 366 °CA are weaker in comparison to ones of the reference OP1. At 367 °CA the signals of the flame luminosity show that the start of reaction is nearly identical to OP1, whereas the LIF image at the same moment expresses a weaker rebound of the vapor phase with a wider expansion along the combustion bowl wall. The transition towards predominantly lean combustion in the outer area of the combustion chamber takes place in accordance with OP1, only the fraction of diffusive combustion regions is noticeable smaller. The detected soot at 370 °CA is

according to the reference at the virtual points of impact of the spray, but as observable on the LII image spatially less distinctive and not that intensive. The subsequent combustion process is, apart from the weaker diffusive part and thus the lower soot signals, practically identical to one of the reference point OP1. The burn-out of the cylinder charge as well as the duration of the combustion is achieved at the same time and crank angle position too. Only the diffusive flame regions at the nozzle tip are more distinctive.

6. SUMMARY

In the context of the project "Spray-Wall Interaction II" the simultaneous optical measuring technique was further improved and the investigations done show that with technique nearly all important processes of the diesel combustion, like injection, spray propagation, evaporation, ignition, combustion and soot emission can be analyzed at the same time. The great advantage of the simultaneous application is the acquisition of the maximum amount of information from one engine cycle without the loss of the complex interactions of the single activities. The results of this research of the influence of the nozzle hole length on the spray behaviour and the subsequent processes can be summarized as follows.

This modification shows shortly after the visible start of injection no significant difference concerning the cone angle and the spray propagation. With increasing injection time this effect becomes more obvious as the break-up of the spray jet is displaced from the nozzle tip and thus the penetration depth is increased. The subsequent evaporation reveals a wider spreading along the combustion bowl wall and a weaker rebound into the combustion chamber. The ignition occurs at the same crank angle position in the middle of the semicircular vapor areas. According to the start of combustion of the reference point OP1 it is also a displacement of the flame regions towards the outer area of the combustion chamber and the formation of a predominately lean combustion ring observable. The appearing sooting regions at the virtual points of impact of the spray on the wall are much lesser developed as well as the rich combustion. Concerning the duration and the end of combustion no significant differences are noticeable; solely the diffusive flame regions at the nozzle tip are vaster.

7. ACKNOWLEDGEMENTS

The authors gratefully acknowledge financial support for parts of their work by the Bundesministerium für Wirtschaft (BMWi, Bonn) and the Arbeitsgemeinschaft industrieller Forschungsvereinigungen (AiF, Köln) as well as by the German National Science Foundation (DFG). The engine investigated was in parts provided by AUDI AG, Neckarsulm, and the nozzles by Robert Bosch GmbH.

8. DEFINITIONS

CA	crank angle	[°]
DI	direct injection	[-]
FL_UV	flame luminosity in the ultra-violet range of light	[-]

FL_VIS	flame luminosity in the visible range of light	[-]
ICCD	intensified charge coupled device	[-]
k	k-factor, conical nozzle shape	[-]
LII	laser induced incandescence	[-]
LIF	laser-induced fluorescence	[-]
Mie	Mie scattering technique	[-]
Nd:YAG	Neodym doped Yttrium-Aluminium-Garnat	[-]
n	engine speed	[min ⁻¹]
OP	operating point	[-]
PAH	polyaromatic hydrocarbon	[-]
Q _{hyd}	rated hydraulic flow	[cm ³ /30s]
RoHR	rate of heat release	[-]
s	cavitation free nozzle hole	[-]
ε	compression ratio	[-]

1. Fettes, C., Leipertz, A., Potentials of a Piezo-Driven Passenger Car Common-Rail System to Meet Future Emission Legislations - An Evaluation By Means of In-Cylinder Analysis of Injection and Combustion, SAE Technical Paper 2001-01-3499, 2001.
2. Taschek, M., Koch, P., Egermann, J., Leipertz, A., Simultaneous Optical Diagnostics of HSDI Diesel Combustion Processes, SAE Technical Paper 2005-01-3845, 2005.
3. Baritaud, T., Optical Measurements in DI Diesel Engines, K. K. Höinghaus, J. B. Jeffries (eds.), Applied Combustion Diagnostics, Tayler and Francis, pp. 431-451, 2002.
4. Leipertz, A., Quantitative Two- and Three-Dimensional Measurement Techniques, D.F.G. Durão et al.(eds.), Instrumentation for Combustion and Flow in Engines, Kluwer Academic Publications, pp. 123-140, 1989.
5. Bertsch, D., Experimentelle Untersuchungen zum Einfluß gemischbildungsseitiger Maßnahmen auf den Zündprozeß, Verbrennung und Schadstoffbildung an einem optisch zugänglichen DE-Dieselmotor, PhD-Thesis, University of Karlsruhe, 1999.
6. Koyanagi, K., et al.: Optimizing common-rail injection by optical diagnostics in a transparent production type diesel engine; SAE Technical Paper 1999-01-3646 1999.
7. Gaydon, A. G., The Spectroscopy of Flames, Champan & Hall, London, 1957.
8. Hultqvist, A. et al., A Study of the Homogeneous Charge Compression Ignition Combustion Process by Chemiluminescence Imaging, SAE Technical Paper 1999-01-3680, 1999.
9. Dec, J., Espey, C., Chemiluminescence Imaging of Autoignition in a DI Diesel Engine, SAE Technical Paper 982685, 1998.
10. Dec, J., Espey, C., Ignition and Early Soot Formation in a DI Diesel Engine Using Multiple 2-D Imaging Diagnostics, SAE Technical Paper 950456, 1995.
11. Santoro, R.: Laser-Induced Incandescence, K. K. Höinghaus, J. B. Jeffries (eds.), Applied Combustion Diagnostics, Tayler and Francis, pp. 252-286, 2002.

12. Leipertz, A., Ossler, F., Alden, M., Polycyclic Aromatic Hydrocarbons and Soot Diagnostics by Optical Techniques, K. K. Höinghaus, J. B. Jeffries (eds.), Applied Combustion Diagnostics, Taylor and Francis, pp. 359-383, 2002.
13. Quay, B., Lee, T.-W., Ni, T., Santoro, R. J., Spatially resolved measurements of soot volume fraction using laser-induced incandescence, *Com. Flame* 97, pp. 384-392, 1997.